Shock Structural Tests for NSRR Experimental Capsule Using Slow Explosive

Sadamitsu Tanzawa, Toshio Fujishiro
Japan Atomic Energy Research Institute, Ibaraki, Japan
Shinji Yoshie, Morihiro Iwasaki
Kawasaki Heavy Industries Ltd., Tokyo, Japan

1 INTRODUCTION

In-pile experiments are being conducted in the Nuclear Safety Research Reactor (NSRR) to study the behavior of fuel rod failure under Reactivity Initiated Accident (RIA) conditions in Light Water Reactors (LWRs). The outline of the NSRR is shown in Figure 1. In the RIA, large excess reactivity is inserted by an inadvertent control rod withdrawal or ejection, resulting in a prompt power excursion of the reactor. The rapid increase of reactor power causes the fuel rod failure.

In the NSRR experiments, a test fuel rod contained in a cylindrical capsule is subjected to a large pulse neutron irradiation in the central test cavity of the reactor and the prompt energy generation of an RIA is realized by nuclear fission of the test fuel. In a most severe test case, the test fuel rod is molten and dispersed into the coolant (water), and generates impulsive pressure. (Fujishiro, 1979) If a free surface exists in the irradiation capsule, a water column above the fuel failure region is blown up and impacts on the plug.

The capsule used in the NSRR is required in safety aspects to maintain its structural integrity under such a shock loading condition. On the other hand, the wall thickness of the capsule should be as thin as possible in order to decrease the absorption of neutrons so that enough energy is deposited in the fuel. In the irradiated fuel tests which are newly planned in the NSRR program, a double-containment capsule should be used to attain high reliability against the leakage of fission products. The decrease of the wall thickness of the inner capsule is more definitely requested from the point of view of neutron absorption. Therefore the adoption of the dynamic elasto-plastic design is planned to permit a certain extent of plastic deformation.

In this context, the authors will report the results of out-pile tests which were conducted to evaluate the dynamic deformation characteristics of the double-containment capsule and to obtain data for analytic code validation for the plastic design. In the tests, a slow-burning explosive was used in water to simulate dynamic loads in the NSRR experiments. In what follows, described are major experimental results and their evaluation of pressure wave propagation, impact pressure behavior depending on the cover-gas volume, and dynamic deformation behavior of the capsule including the comparison between a uni-capsule and a double capsule structure.

2 EXPERIMENTAL PROCEDURE

2.1 Experimental Models

Figure 2 shows a double capsule which consists of an inner vessel and an outer vessel. In the single-containment capsule (hereinafter called "uni-capsule") tests, the inner vessel of the double capsule is used single-handed. The scale of the model is the same as the NSRR irradiation capsule and water is used as the coolant. The inner vessel is hung down from the underside of the upper plug of the outer vessel with the help of three hanger rods. Both the uni-capsule and the double capsule were used in the tests. The above models were made of the same stainless steel type 304 as the actual capsule and the tests were performed at room temperature.

In addition to these capsule models, a thick-walled (rigid) vessel, that would be free from plastic deformation due to dynamic pressure, was used for energy calibration and examination of effects of cover-gas volume.

2.2 Energy Source

A slow-burning explosive ($KClO_4$: 72%, Al: 28%; density: 1.63 g/cc) was used as an energy source to simulate the dynamic loads expected at fuel rod failure. The explosive was placed in the center of the inner vessel and the capsule was tightly closed including cover-gas (air). The pressure waves as a target energy source were 20 to 40 MPa at peak and the duration time was about 1 ms.

2.3 Instrumentation

The locations of pressure transducers and strain gages are shown in Figure 3. To examine the deformation profile, marker lines were drawn on the surfaces of the deformable part (wall thickness: 4.5 mm) of the capsule. The velocity history of the water column above the explosive (hereinafter called "slug") was measured with a floating magnetic sensor, a combination of a coil and a permanent magnet, placed in the cover-gas of the closed rigid vessel. Further, the slug velocity in the open rigid vessel was directly measured by the use of a high-speed camera. In this case, the compression effect of cover-gas did not exist.

3 TEST RESULTS AND DISCUSSION

3.1 Rigid Vessel Tests

(1) Pressure Wave Propagation

The standard test conditions and the pressure history at main points are shown in Figure 4. At P2 near the energy source, a pressure wave which has 20 MPa at peak with 1 ms in width including reflection was observed. The pressure wave emitted from the energy source propagates in the axial direction and is reflected by the boundary between the free surface and the bottom wall of the vessel. P6 represents the slug impact pressure including the compression of cover-gas. The slug velocity at impact was about 50 m/s, which was calculated backwards from the rising time of impact pressure Ⓓ at P6 in Figure 4.

Figure 5 shows a typical state of wave propagation. The initial peak pressure of the wave Ⓐ of P4 shows a doubled value of the peak pressure of the energy source due to the rigid wall reflection. So the peak pressure of the energy source can be estimated by measuring the pressure at the position P4. The rising time of the second pressure wave at P4 is estimated as Ⓑ and Ⓒ in the Figure.

(2) Slug Velocity History

The slug velocity is necessary to estimate the kinetic energy of slug. Figure 6 shows an example of the slug velocity history in the standard test conditions. The pressure wave near the energy source was at a level of 10 MPa with 1 ms in this case. Shown in the figure is the comparison between the measurements when the vessel is hermetically sealed and when the vessel is kept open. Both cases show almost identical histories, and the effect of the compressibility of the cover-gas on the slug velocity is deemed to be small in this test condition. As described in the next paragraph, however, the compressibility is an important factor to find the slug velocity when the cover-gas height is small and the energy source level is relatively high.

(3) Effects of Cover-gas Height

In the tests, the distance between the explosive and the free surface was kept constant (200 mm) so that the slug quantity would be constant, while the cover-gas height (δ) was changed from 50 to 250 mm. The peak pressure of the energy source was set at a level of 20 MPa.

The pressure history at each point in both cases is shown in Figures 7 and 8. As shown by the first peak pressure of P6, the compression effect of the cover-gas in the case of δ=50 mm is larger than in the case of δ=250 mm. The relationships among the cover-gas height, slug velocity and slug impact pressure are determined by the balance between the released history of source energy and the elastic response of the cover-gas. It is predicted from the above results that the deformation possibility of the upper part of the capsule in the case of small cover-gas volume becomes larger when the same source energy is given.

If the cover-gas height is small, namely δ=50 mm, cover-gas condition converts in early stage from the compression process to the expansion process, and the slug bouncing phenomenon generates a secondary slug impact pressure on the lower part of the water. (See P4, Ⓔ in Figure 7)

The rigid vessel tests indicated that the pressure wave with larger peak pressure appeared in the lower and the upper part of the vessel and that the smaller volume of cover-gas resulted in the higher peak pressure in the upper part of the vessel if the energy source was the same.

3.2 Capsule Tests

Both in the uni-capsule test and the double capsule test, the explosive was located 200 mm above the bottom of the inner vessel and the free surface was 200 mm above the explosive. This test condition was identical to that of the standard case in the rigid vessel test. In the capsule tests, the charge of explosive was increased so that the capsule would deform to a meaningful extent for the code validation.

The pressures measured in both capsule tests were very similar to each other at the bottom of the capsule (P4) and on the underside of the plug (P6). Since the energy source level was the same (See Figures 9 and 10.), the difference in dynamic deformation behavior in both tests can be extracted.

(1) Uni-capsule test

The strain history at each point is shown in Figure 11. Due to the elastic deformation in the radial direction of the capsule near the energy source, the tensile stress wave propagates in the axial direction, so tensile behavior is observed at Ⓕ by S2 (axial) while compressive behavior at Ⓖ by S1 (circumferential). When the pressure wave reached the bottom of the capsule,

tension is observed again at Ⓗ by S2 and compression at Ⓘ by S1. In about 2.5 ms after explosion, in response to the slug impact, tension is observed at Ⓙ by S1 in the Figure 11. Even though the slug impact pressure was over 120 MPa, the upper part of the capsule was not deformed because the upper part was built relatively thick.

The maximum deformation occurred at S8 and S9 at the bottom of the capsule in response to the reflected pressure wave at P4. In this part, the deformation remained both in circumferential and axial directions, and the plastic circumferential strain was about 1.1 percent. As the strain history at S8 shows, the deformation was formed in two stages. In the first stage, the deformation shown at Ⓚ in Figure 11 is generated by the initial pressure wave from the energy source, and in the second stage (Figure 11, S8, Ⓛ), it was generated by the reflected wave from the bottom of the capsule. The strain was thus built up. The changes of strain rates indicated by Ⓚ and Ⓛ correspond to those of respective pressure wave.

(2) Double capsule test

The pressure history and the strain history are shown in Figures 10 and 12, respectively. The deformation behavior of the inner vessel is basically the same as that of the uni-capsule. However, as shown by S8 in Fig. 12, the plastic circumferential strain was about 0.8 percent, which was smaller by around 30 percent in comparison with the uni-capsule. Such a mitigating effect is explained by the existence of fluid (water) in the annulus between the inner and the outer vessel wall, which caused the equivalent thickness of capsule wall to increase and the outer vessel wall to share a certain amount of the deformation.

4 CONCLUSIONS

(1) The correlations among the cover-gas height, the slug velocity, the slug impact pressure and the compression effect were quantitatively obtained. It was revealed that the secondary impact pressure resulted from the slug bouncing due to the elastic behavior of cover-gas.

(2) The dynamic deformation characteristics of the uni-capsule was evaluated in relation to the pressure wave propagation behavior in the water.

(3) It was experimentally confirmed that the fluid in the annulus section and the outer vessel mitigate the deformation of the inner vessel quantitatively.

(4) The fundamental data of the shock structural characteristics were obtained for a code validation.

ACKNOWLEDGEMENT

The authors are deeply indebted to Dr. K. Tanaka, former principal researcher, in the National Chemical Laboratory for Industry, Agency of Industrial Science and Technology, for his guidance in the measurement of impulsive pressure and the interpretation of it's propagation.

REFERENCE

T. Fujishiro, et al., (1979). A Study on Pressure Generation Caused by Actual Fuel Failure in the NSRR Experiment. Fourth CSNI Specialist Meeting on Fuel - Coolant Interaction in Nuclear Reactor Safety, Bournemouth, UK

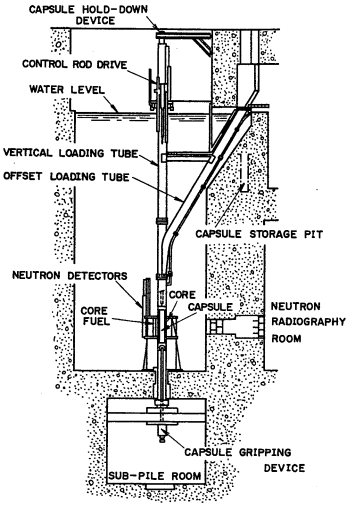

Fig. 1 Cross-section of NSRR

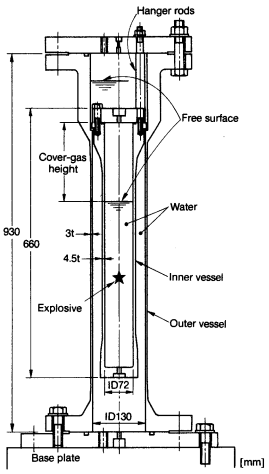

Fig. 2 Capsule model

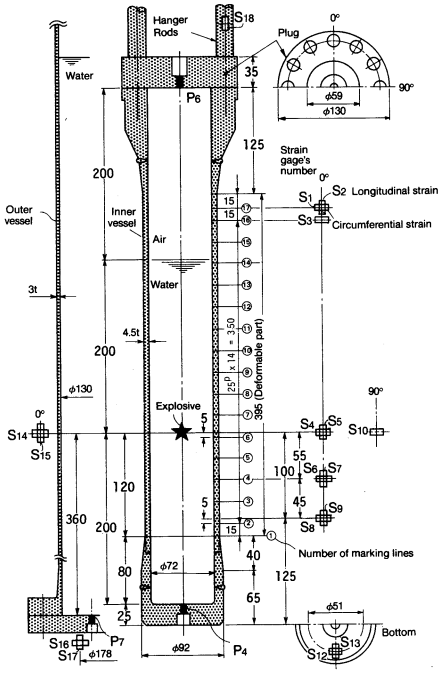

Fig. 3 Location of pressure transducer & strain gage

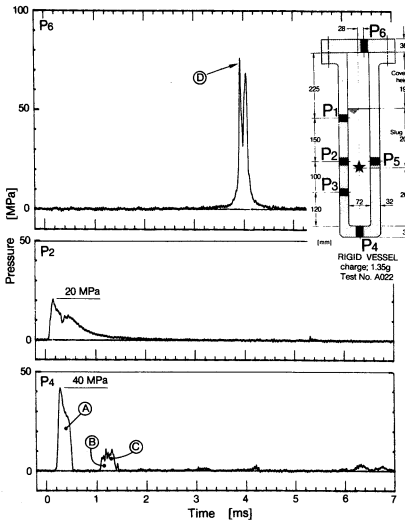

Fig. 4 Pressure history for standard case

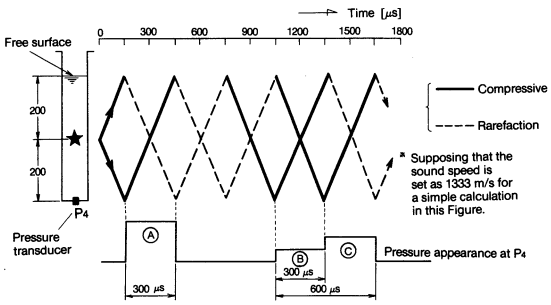

Fig. 5 Illustration of presure wave propagation

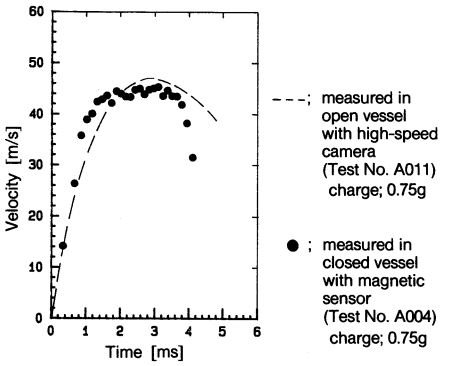

Fig. 6 Slug velocity history

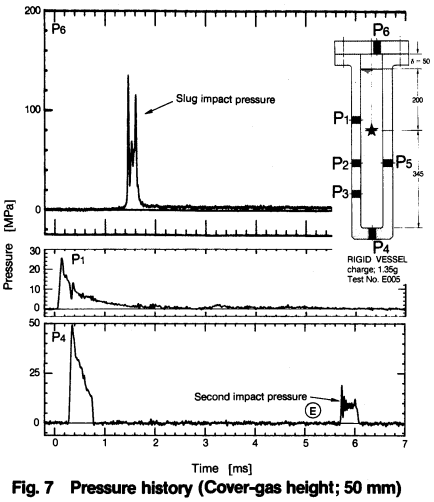

Fig. 7 Pressure history (Cover-gas height; 50 mm)

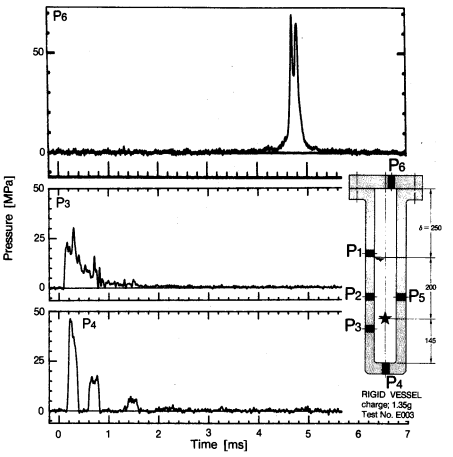

Fig. 8 Pressure history (Cover-gas height; 250 mm)

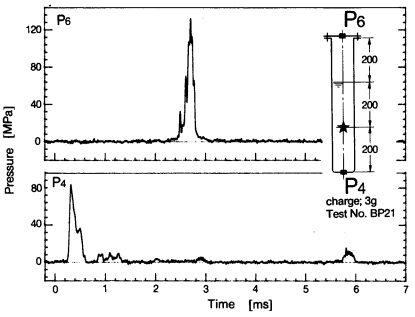

Fig. 9 Pressure history of uni-capsule

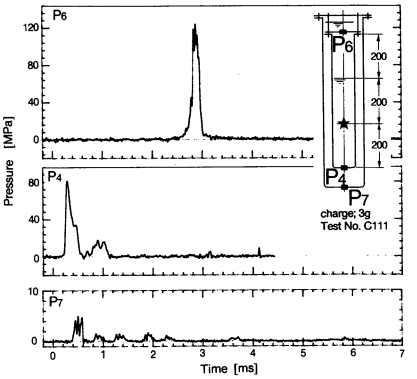

Fig. 10 Pressure history of double capsule

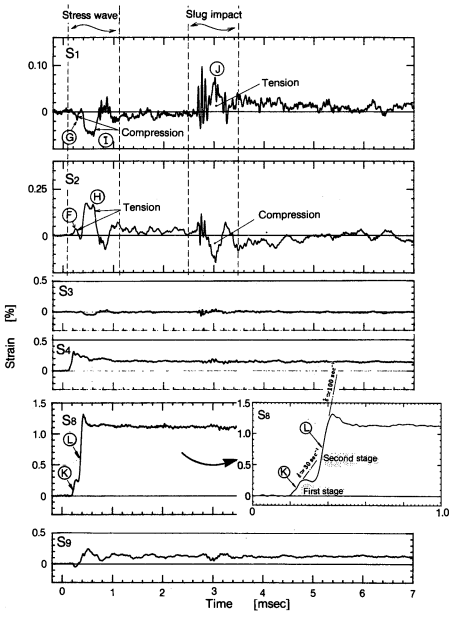

Fig. 11 Strain history of uni-capsule [Test No. BP21]

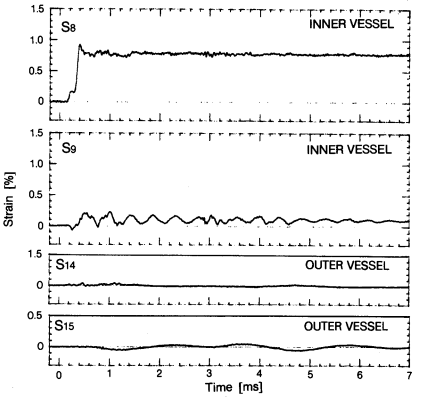

Fig. 12 Strain history of double capsule